LABORATÓRIO DE INSTRUMENTAÇÃO
E FÍSICA EXPERIMENTAL DE PARTÍCULAS
partículas e tecnologia

Best Poster competition

Best Poster in Particle Physics - **Souvik Priyam Adhya**

Best Poster in Nuclear Physics - **Maud Versteegen**

Best Poster in Instrumentation - **Fabio Happacher**

Best Poster authored by a PhD Student - **Ingo Rienäcker**

CONGRATULATIONS!

CERTIFICATE

BEST POSTER AWARD
IN PARTICLE PHYSICS

PANIC Lisbon Portugal
Particles and Nuclei International Conference

This certificate is given to

Souvik Priyam Adhya

"PANIC 2021", organized by LIP, Lisbon, Portugal between September 5th and 10th 2021, online.

Mário Pimenta
LIP President

Helena Santos
Conference Chair

CERTIFICATE

BEST POSTER AWARD
IN NUCLEAR PHYSICS

PANIC Lisbon Portugal
Particles and Nuclei International Conference

This certificate is given to

Maud Versteegen

"PANIC 2021", organized by LIP, Lisbon, Portugal between September 5th and 10th 2021, online.

Mário Pimenta
LIP President

Helena Santos
Conference Chair

CERTIFICATE

BEST POSTER AWARD
IN INSTRUMENTATION

PANIC Lisbon Portugal
Particles and Nuclei International Conference

This certificate is given to

Fabio Happacher

"PANIC 2021", organized by LIP, Lisbon, Portugal between September 5th and 10th 2021, online.

Mário Pimenta
LIP President

Helena Santos
Conference Chair

CERTIFICATE

BEST POSTER AWARD
AUTHORED BY A PHD STUDENT

PANIC Lisbon Portugal
Particles and Nuclei International Conference

This certificate is given to

Ingo Rienäcker

"PANIC 2021", organized by LIP, Lisbon, Portugal between September 5th and 10th 2021, online.

Mário Pimenta
LIP President

Helena Santos
Conference Chair

RWTH AACHEN UNIVERSITY · JEDI · JÜLICH Forschungszentrum

The Search for Electric Dipole Moments of Charged Particles in Storage Rings

Achim Andres for the JEDI Collaboration - RWTH Aachen University & Forschungszentrum Jülich

Physics Motivation

Electric Dipole Moments (EDMs)

- Fundamental (vector) property of a particle aligned with the particles spin axis
- Requires $\mathcal{P}$ and $\mathcal{T}$ or $\mathcal{CP}$ violation
- **Basic Idea:** Measure influence of EDM on beam polarization
- COSY: Magnetic ring → Horizontal polarization precesses ($\vec{P}_t$) around **invariant spin axis** $\hat{n}$
- Non-zero EDM tilts $\hat{n}$ in radial (x) direction
- Determination of the orientation of $\hat{n}$ gives access to $\vec{d}$

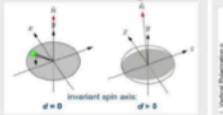

- However, ring imperfections (magnet misalignments,..) also lead to rotations of $\hat{n}$ in radial and longitudinal direction
- **Siberian Snake** adds polarization rotation (ζ^{Snk}) in **longitudinal direction** and is therefore used to measure longitudinal (z) component of $\hat{n}$
- **RF Wien Filter** operating on the spin precession frequency ($\vec{\Omega}$) loading to a rotation of the polarization in **radial direction** (x) by a rotation of the device around the beam pipe ($\vec{\omega}^{\text{WF}}$)

Technique

- Fix Wien Filter $\vec{\omega}^{\text{WF}}$ and Siberian Snake ζ^{Snk} rotation angle
- Measurement repeated for 31 different settings of Wien Filter and Siberian Snake
- Determine the initial slope of vertical polarization after switching on the RF Wien Filter and the Siberian Snake at 155 s in the Cycle
- Beam polarization is determined by scattering the particle beam onto a accelerator internal polarimeter (JePo - Jedi Polarimeter)

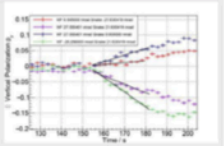

Figure: Build-up of the vertical polarization for different settings of the RF Wien Filter and the Siberian Snake

EDM resonance strength ϵ^{EDM} is given by the slope of the increasing vertical polarization

$$\epsilon_{\text{EDM}}(\vec{\omega}^{\text{WF}}, \zeta^{\text{Snk}}) \sim \vec{\beta}_t$$

Preliminary Results - Precursor I

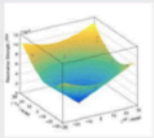

$$\epsilon^{\text{EDM}}(\vec{\omega}^{\text{WF}}, \zeta^{\text{Snk}}) = \left[A^2_{\text{hor}} \left(\vec{\omega}^{\text{WF}} - \vec{\omega}^{\text{WF}}_0 \right)^2 + A^2_{\text{ver}} \left(\frac{\zeta^{\text{Snk}} - \zeta^{\text{Snk}}_0}{2 \sin\left(\pi f_s / f_{\text{rev}}\right)} \right)^2 \right]^{\frac{1}{2}}$$

Orientation of invariant spin axis $\hat{n}$ including ring imperfections is experimentally given by the minimum of the paraboloid [1]

$$\vec{\omega}^{\text{WF}}_0 = -2.91(8)\,\text{mrad}$$
$$\zeta^{\text{Snk}}_0 = -5.22(7)\,\text{mrad}$$

- Minimum represents spin rotation axis **including** EDM
- Simulated spin tracking shall determine orientation of stable spin axis **without** an EDM
- EDM limit is determined from the difference of 1. and 2.

References

[1] F. Rathmann, N. Nikolaev, and J. Slim, *Spin dynamics investigations for the electric dipole moment experiment*, Physical Review Accelerators and Beams, 23 (2020).

Contact: Achim Andres - a.andres@fz-juelich.de

Member of the Helmholtz Association

PANIC Lisbon Portugal
Particles and Nuclei International Conference

Modeling the radiobiological effects of gold nanoparticles in proton therapy of glioblastomas

Joana Antunes, Jorge Miguel Sampaio, Filipa Mendes, António Paulo

MOTIVATION

The combination of high-Z nanoparticles (NP) and external radiotherapy leads to an increased radiation effect in tumoral cells without an increase of the patient dose (Figure 1).

However, it is not yet clear how the sequence of physical, chemical, and biological mechanisms contributes to the observed synergic effect.

Figure 1. Effect of NPs in tumoral cells [1].

OBJECTIVE

Develop realistic simulations of the irradiation of monolayer (2D) and spheroid (3D) human glioblastomas multiforme (GBM) cell cultures, taking into consideration different concentrations and cellular distributions of the gold nanoparticles (GNPs).

TOol for PArticle Simulation

The simulations will be implemented based on TOPAS [2] software more specifically the extension TOPAS-nBio [3] that includes models of the physical and chemical processes induced by radiation at the DNA scale.

Figure 2. a) TOPAS e b) TOPAS-nBio

METHODOLOGY

To built the simulation is necessary define four sections:

Geometry

The construction of the computational cell models will be developed based on confocal microscopy images of the biological samples.

Source

We simulate irradiations with different types of radiation:

- X-ray spectra with 50 and 150 kVp
- Cobalt-60 beam
- Proton beam with 80 keV, 18 MeV and 150 MeV

Physics List

To simulate the physical interactions, we define two different lists:

- Geant4-DNA list
- Livermore list

We also include in the simulations the production of fluorescence and auger electrons, the Auger Cascade and the PIXE process.

Output

The dose distributions at the subcellular scale will be obtained, as well as the temporal distribution of the reactive oxygen species (ROS).

RADIOBIOLOGICAL MODELS

The simulations outputs will be used to predict cell survival fractions (S), using standard mathematical models of the biological effects of radiation as Local Effect Model (LEM) and Microdosimetric Kinetic Model (MKM) [4]. Both models assume that the cell nucleus is the principal target, and it is divided into small independent domains. The application of this models to GNP radio-enhancement is done considering the probability of interaction (p) and the radial dose per ionization from single GNP (d_{GNP}).

LEM

The number of lethal events ($\bar{L}_n$) is a function of the absorbed dose in infinitesimally small volume in the nucleus (d):

$$\bar{L}_n(d) = \begin{cases} \alpha d + \beta d^2, & d \le D_t \\ (\alpha + 2\beta D_t)d - \beta D_t^2, & d > D_t \end{cases}$$

$$d = D(1 + p\, d_{GNP}) \qquad S = \exp(-(\bar{L}_n(d)))$$

MKM

The number of lethal events ($\bar{L}_n$) depends on the average absorbed dose in the nucleus ($\bar{D}_n$) and on the dose-mean linear energy ($\overline{LE}$):

$$(\bar{L}_n(\bar{D}_n)) = \alpha^* \bar{D}_n + \beta \bar{D}_n^2 \qquad \alpha^* = \alpha + \frac{\beta \overline{LE}}{\rho \pi r_d^2}$$

$$\bar{D}_n = \frac{\sum_{i=1}^{N} D(1 + p(d_{GNP})_i)}{N}$$

$$S = \exp(-(\bar{L}_n(\bar{D}_n)))$$

RESULTS

The results obtained in the simulations will be compared with the biological in vitro and in vivo experimental results, which will include evaluation of cell viability and survival. Moreover, the simulated ROS yields will be also compared with the experimentally determined values.

So far, we did the definition of geometry on TOPAS, represented in figure 3c.

In the future, we will use this complex and realistic geometry to obtain more accurate results when compared to those obtained when using simple geometries.

Figure 3. a) Original image b) segmented image c) Geometry defined on TOPAS